Adhesion characterization of SiO_2 thin films evaporated onto a polymeric substrate

C. Ho[1], A. Dehoux[2], L. Lacroix[3], J. Alexis[4*], O. Dalverny[5], S. Châtel[6], B. Faure[7]

[1,3,4,5]Department of Interfaces and Functional Materials, LGP-ENIT-INP, University of Toulouse, France
[1,2,6,7]Thin Films Group, R&D Physico-Chemistry, Essilor International, France

***Abstract*—** *To ensure good adhesion between a 200 nm thick silicon dioxide layer and a 4.5 µm thick hardcoat polymeric coating, a better understanding of mechanisms of adhesion at this interface is needed. To reach this purpose, focus is placed on two axes: characterizing mechanical properties of materials composing the system and in parallel, finding an applicable and effective method to quantify adhesion. Small dimension of SiO_2 thin film makes it challenging to accurately characterize it. Hence the use of both nano-indentation and AFM to attempt assessment of SiO_2 thin film elastic modulus Ef; taking into account limitations and uncertainty associated with each technique. Elastic modulus of SiO_2 thin film determined by nano-indentation is roughly 50 GPa on a wafer substrate and 15 GPa on a lens substrate. As for AFM, modulus measured is approximately 56 GPa on a wafer substrate and 22 GPa on a lens substrate. This highlights significant influence of substrate for both techniques. Impact on mechanical properties between SiO_2 thin films under different intrinsic stresses was also investigated. Results suggest that higher density of SiO_2 thin film leads to higher elastic modulus.*

To quantify adhesion, micro-tensile and micro-compression tests were performed. Micro-tensile experiments give ultimate shear strengths of hardcoat-substrate interface ranging from 9 to 14 MPa. Values of energy release rates of SiO_2 / Hardcoat, range from 0.1 J/m² to 0.5 J/m², depending on moduli values found on wafer or lens substrate.

***Keywords*— Adhesion, mechanical properties, oxide thin film, polymer substrate.**

I. INTRODUCTION

Ophthalmic lenses are made of plastic polymeric substrates usually coated with functional treatments composed of 5 to 15 layers, ranging from micrometers to nanometers. The first treatment consists of a primer, conferring impact resistance properties to the lens. A hardcoat with nanoparticles, is then deposited on top of this primer, bringing anti-scratch properties to the system. Both primer and hardcoat are within the micrometer scale and are deposited by wet chemical methods. Nanometric anti-reflective stacks are then evaporated onto the hardcoat by vapor deposition technology, to enhance wearers' comfort. Interface quality is essential to ensure stability and durability of ophthalmic multi-layer. In fact, insufficient adhesion between layers causes higher susceptibility to emergence of defects or delamination. Occurrence of these phenomena affects wearers' comfort and has tremendous impact on products' lifetime. Therefore, it is essential to develop a method enabling quantitative assessment of interface quality, which will ultimately enable to ensure high product reliability.

General behavior of whole system must be fully characterized. To reduce the complexity of this characterization, focus is first placed on studying the interface between the anti-reflective stack and the hardcoat. More specifically, this paper centers around the SiO_2 thin film / hardcoat interface, which is particularly sensitive because of mechanical and dimensional contrast between SiO_2 thin film and hardcoat.

This entails studying both materials composing each layer and interface. Interface quality can be evaluated through quantification of adhesion energy. Over 300 adhesion tests are referenced in the literature [1]. Choice of appropriate method to access adhesion is made according to compatibility with system under study, repeatability, ease of implementation, cost effectiveness and representativeness of defects observed in real life versus defects generated by mechanical tests. Techniques commonly used on similar structure - rigid thin film of 200 nm on soft substrate - include Superlayer, Laser adherence test (Lasat), Bulge test, Pull-off test, three-point bending, micro-tensile and micro-compression tests. Superlayer adhesion test [2], consisting in depositing a highly stressed layer on top of interface of interest, is examined. Lau [3] determines interfacial fracture toughness ranging from 12 J/m² to 24.5 J/m² for dry samples of 0.9 µm silica on 20 µm epoxy, using stressed Chrome Superlayer. Several attempts to generate spontaneous delamination of studied SiO_2 thin film using a Zirconium Superlayer were ineffective. This attests a strong adhesion at SiO_2 / Hardcoat interface. Mechanical test generated by acoustic shock wave, Lasat [4], Bulge test [5] were considered but have not been implemented. Indeed, Lasat test involves laser shock wave that is likely to alter soft polymeric substrate and therefore, is inadequate to structure being studied. Bulge test requires etching step which is delicate considering small dimensions at stake. Moreover, presence of similar chemical

elements between thin film and substrate makes selectiveness of etching process even more complex, which makes bulge test hardly applicable on structure under study. Pull-off tests and three-point bending experiments have been performed. Results located weakest interface at SiO_2 thin film / stiffener and SiO_2 thin film / adhesive interface respectively. This exposes challenge of finding appropriate stiffener or adhesive for strong adhesion interface. This is the reason why pull-off tests and three-point bending experiments were not favored. Through micro-tensile experiments, Alexis et al. [6, 7] have shown correlation between talc particles proportion, thermal post-treatments and practical adhesion of NiP-talc on steel. These results suggest that mechanical adhesion of NiP-talc on steel increases as a function of talc particles proportion and thermal post-treatments. Using micro-compression tests, Xue [8] shows emergence of buckles in a 200 nm titanium thin film sputtered on PMMA substrate. Mode I and Mode II toughness of 0.2 J/m^2 and 0.8 J/m^2 respectively, and interface strength of 80 MPa were determined for Ti / PMMA system by finite element simulations. Considering specifications required for choice of adhesion test and preliminary testing, focus was placed on both micro-compression and micro-tensile tests, which seems suitable for system being studied and have the advantage of applying uniaxial stress without mechanical contact in the area under observation.

As mentioned earlier, emphasis is also placed on determining mechanical behavior of each material to obtain a global understanding of the composite system being studied. In fact, regardless of the adhesion test performed, mechanical properties are needed to fully understand fracture energies. More specifically, it is important to quantify contributions of elastic and plastic dissipations, as well as dissipations through friction or fracture, to estimate adhesion at interface as accurately as possible. Nano-indentation [9] is widely used to determine mechanical properties of both bulk materials and thin films deposited on substrate. However, influence of substrate is inevitable for thin films of a couple of nanometers thick. To limit this effect, correction of substrate's influence using FEA exists [10, 11]. Another approach consists in using an alternative technique with better surface detection to enable characterization of the first nanometers of thin film. AFM, one of the best techniques for surface imaging at an extremely high resolution, classically gives topography and surface roughness information. Nevertheless, several studies have used AFM to extract mechanical properties of sample of interest. Elastic modulus can indeed be determined using DMT contact model with slope of retract curve [12, 13]. As mentioned earlier, this alternative method to characterize elastic modulus has the advantage of having higher sensitiveness to surface detection compared to nanoindentation. It also involves a more confined interaction volume, which is expected to lead to a lower impact from the film microstructure or the substrate. However, limitations of mechanical characterization by AFM include sensitiveness to topography, cantilever spring constant and tip contact area uncertainties. In the present study, elastic modulus of SiO_2 thin film deposited on Si wafer and ophthalmic lens substrate are characterized by both nano-indentation and Peak Force AFM. Micro-tensile and micro-compression results to quantify SiO_2 / hardcoat adhesion, are also presented.

II. MATERIALS AND METHODS

2.1 Samples

SiO_2 Type A and SiO_2 Type B are deposited by evaporation under vacuum whether on silicon wafer (280 µm thick and 2 inches diameter wafers) or on top of standard ophthalmic structure: 4.5 µm composite polymer referred to as hardcoat, on a 2 mm polycarbonate substrate. That is a total of four sample configurations, represented in Figure 1. Deposition of both types of SiO_2 layers is conducted under a pressure of 8.10^{-5} to 1.5×10^{-4} mbar [14]. Difference between SiO_2 Type A and B results from supply of gas during deposition: SiO_2 Type A is deposited along with oxygen gas whereas SiO_2 Type B deposition does not involve introduction of additional gas. This difference in process was proven to effectively generate different levels of intrinsic stress within SiO_2 layers, due to increase of porosity related to gas scattering during deposition [15]

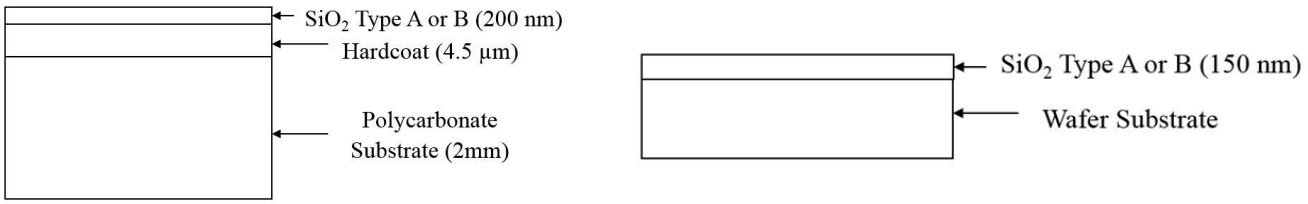

(a) **(b)**

FIG. 1. Representation (not to scale) of sample configurations on lens substrate (a) and silicon wafer substrate (b).

Compressive intrinsic stress of SiO_2 Type on glass strip (60 mm x 5 cm x 150 µm) was measured to be roughly -100 MPa, compared to -400 MPa for SiO_2 Type B. Bending curvature of glass strip was measured before deposition of SiO_2 thin film on KLA Tencor P16+. Glass strip was then placed into evaporation under vacuum chamber (glass strip being only clamped on one end, the other end remaining free) to receive deposition of SiO_2 thin film. Another measurement of glass strip's bending curvature was performed 2 hours after deposition. Compressive intrinsic stresses are then calculated using Stoney's equation [16, 17]. Stoney uses bending curvature of glass strip before and after deposition of SiO_2 thin film.

$$\sigma_f = -E_s \frac{{h_s}^2}{(1-\nu_s)h_f}\frac{1}{R} \tag{1}$$

Where E_s is Young modulus of substrate, h_s and h_f are substrate and film thickness respectively, ν_s is substrate's Poisson coefficient and R is radius of curvature. Presented below are methods used to characterize materials mechanical properties, by nano-indentation and AFM.

2.2 Nano-indentation

Four sample configurations were characterized with a Nanoscope XP III from MTS, using a DCM measuring head and Berkovich diamond tip. A matrix of 30 indents separated by 30 µm, was created for each configuration. Before carrying out nano-indentation tests, tip area was first calibrated with a sample of fused silica. Continuous Stiffness Mode (CSM) which consists in overlapping a small amplitude oscillation at 75 Hz to a load controlled system was used. Using Oliver and Pharr model [9], both elastic modulus and hardness can be extracted directly from nano-indentation curve, plotting load versus displacement into surface.

$$S_e = \frac{2}{\sqrt{\pi}} E_r \sqrt{A(h_c)} \tag{2}$$

Where S_e is contact stiffness determined at the beginning of unloading curve, $A(h_c)$ is contact area as a function of indentation depth and E_r is reduced modulus, expressed as followed:

$$\frac{1}{E_r} = \frac{1-\nu^2}{E} + \frac{1-{\nu_i}^2}{E_i} \tag{3}$$

Where E_i and ν_i are respectively indenter's modulus and Poisson coefficient. A value of 0.18 [18] was taken as silica thin film's Poisson coefficient.

2.3 AFM

Four sample configurations were characterized by AFM using Peak Force QNM mode on a Bruker's Dimension Icon. AFM tip radius has been calibrated using fused silica of known elastic modulus. Cantilever's spring constant of 436 N/m has been given by tip provider. Cantilever with high spring constant has been chosen for its suitability to hard materials. Several Peak Force values have been tested to determine the optimal Peak Force to apply on this specific sample. Using DMT model [19, 20], elastic modulus can be determined with slope of retract curve, Poisson coefficient of film, radius of indenter R and indentation depth δ.

$$F - F_{adh} = \frac{4}{3}\frac{E}{\left(1-\upsilon^2\right)}\sqrt{R}\,\delta^{\frac{3}{2}} \tag{4}$$

Second part of this study involves characterization of practical adhesion of SiO_2 / Hardcoat interface, by micro-tensile and micro-compression test.

2.4 Micro-tensile Test

Micro-tensile test is commonly used to determine material's elasticity, plasticity and toughness properties. Applying Agrawal and Raj's model [21, 22], micro-tensile test can also be used as an adhesion test to determine ultimate shear strength of the interface.

SiO_2 Type A and SiO_2 Type B deposited on top of standard ophthalmic structure were tested. Although interface of interest is SiO_2 / Hardcoat, small dimension of hardcoat hinders testing the bilayer system by itself; hence the use of a 2 mm thick

polymeric substrate to support this structure. Typical tensile specimen was designed, with optimized shoulders and gage length, (Figure 2) to fit Deben's micro-tensile stage (5kN tensile compression and horizontal bending stage) and allow sufficient observation area. Samples were precision machined on a Charly Robot milling machine, with a 2 mm diameter milling cutter.

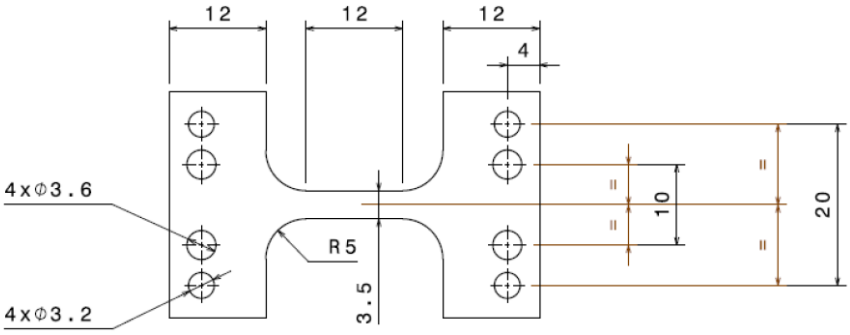

FIG. 2. Representation of tensile specimen

High crack density is associated with good mechanical strength, resulting in higher values of maximal interfacial shear stress τ. Agrawal and Raj [21] relate maximal interfacial shear stress τ with coating thickness, sum of true stress and residual stress σ and maximum cracking spacing λ, when crack density becomes constant.

$$\tau = \frac{\pi h \sigma}{\lambda} \tag{5}$$

2.5 Micro-Compression Test

Configuration of SiO_2 Type B on lens structure sample was tested. Micro-compression tests were performed on the same Deben stage with a 5 kN load cell, used under compression mode. Motor speed was set to 0.2 mm/min. Preliminary tests were performed to estimate minimum deformation of substrate to generate buckling on sample SiO_2 B. 10% deformation and stress of 100 MPa have been proven to be sufficient to buckle studied SiO_2 thin film. Dimensions (Length: 15 mm, Width: 5 mm, Thickness: 2 mm) were then optimized by analytical calculations to avoid flexural buckling of substrate at applied loads, and thus ensuring uniaxial compressive stress. The critical compressive biaxial stress at the onset buckling is expressed as followed:

$$\sigma_{B0} = \frac{\pi^2}{12} \frac{E_f}{1-\nu^2} \left(\frac{h}{b}\right)^2 \tag{6}$$

Where h is thickness of film, is b is half width of buckle and E_f is plane strain moduli of film [23]. Energy release rate G along the sides of the buckle can be estimated by studying on one hand, the average energy per area in the unbuckled state U0 and on the other hand, the average energy per area in the buckled state U, through the relation: $G = U_0 - U$. Expressed differently the energy release rate G is the energy per area needed to separate SiO_2 thin film from substrate over the width of buckle and is defined as [23]:

$$G = G_0 \left(1 - \frac{\sigma_{B0}}{\sigma_0}\right)^2 \tag{7}$$

with G_0, the available energy per area stored in the unbuckled film:

$$G_0 = \frac{(1-\nu_f{}^2)\sigma_0^2 h}{2E_f} \tag{8}$$

With σ_0, the biaxial compressive stress in the buckled plate.

III. RESULTS AND DISCUSSION

3.1 Nano-hardness and rigidity

As shown in Figure 3a, modulus of hardcoat is measured to be between 6 – 7 GPa by nano-indentation. It can be noted that modulus is relatively stable over a wide range of indentation depths; except for the first 10 nm, where surface detection can

be particularly sensitive on a composite polymer. On the contrary, rapid evolution of modulus of SiO_2 thin film as a function of displacement into surface is observed.

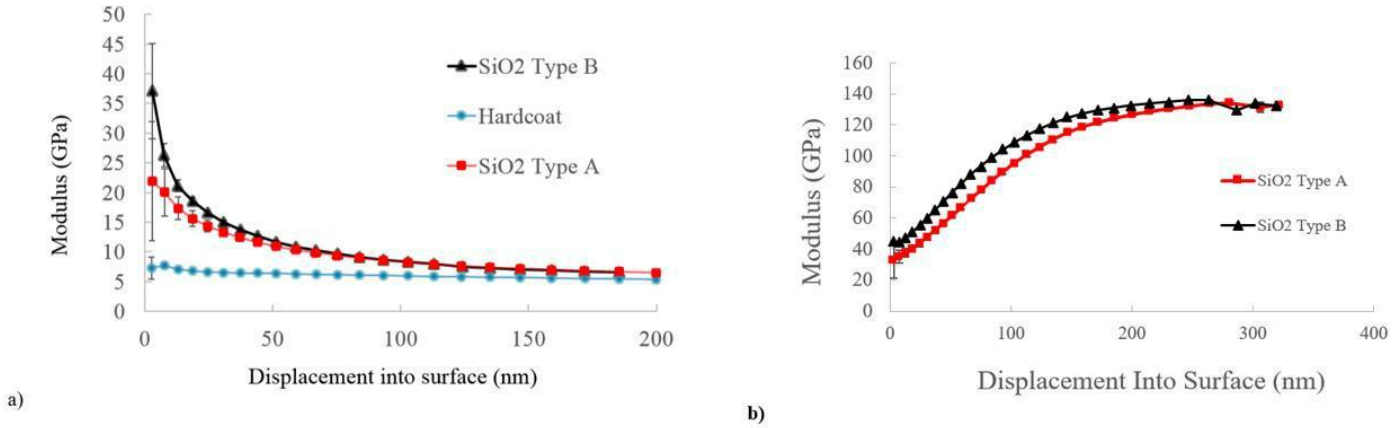

FIG. 3. Representation of their moduli as a function of displacement into surface. (a) Nano-indentation results of Hardcoat, SiO_2 Type A and B deposited on Hardcoat (b) Nano-indentation results of SiO_2 Type A and B on Silicon Wafer

This confirms that substrate's influence has a considerable impact on SiO_2 thin film's modulus measurement. Models to correct substrate's impact relying on FEA to precisely determine contact radius, have not been implemented as it requires mechanical properties of material to characterize. It should be noted that moduli obtained for indentation depths below 20 nm are susceptible to surface detection errors. Above 30 nm indention depth, substrate's influence becomes significant. Moduli are therefore averaged for indentation depths between 20 and 30 nm, even though influence of substrate is already existent and acknowledged (Table 1).

TABLE 1
ELASTIC MODULI OF SiO_2 TYPE A AND B DEPOSITED ON WAFER AND ON OPHTHALMIC LENS, OBTAINED BY NANO-INDENTATION

Substrate	Young Modulus (GPa) SiO_2 A	Young Modulus (GPa) SiO_2 B
Silicon Wafer	46±2	5±1
Ophthalmic lens (hardcoat on Polycarbonate)	14±1	17±0

On both Si wafer and lens substrates, SiO_2 Type A and B are differentiable. Modulus of SiO_2 Type B is 26% higher than modulus of SiO_2 Type A on Si wafer. The same trend is observed for lens substrate, difference being slightly lower (16%). This suggests that the change of material density leads to a higher intrinsic stress and also to the modification of mechanical properties. This is in good agreement with the fact that intrinsic stress is linked to local density – without porosity taken into account - through Si-O-Si deformation; diminution of bond angle at the O atom site, being related to increase in intrinsic stress [15]. Moduli of SiO_2 thin film measured on Si wafer are significantly higher (~250%) than those on lens. According to curves presented on Figure 3, elastic moduli of SiO_2 are overestimated on Si wafer and underestimated on lens substrate. Aside from contribution of substrate's influence, outgassing of lens substrate may explain lower moduli compared to those found on Si wafer. Moreover, during deposition, thermal stress could be generated on polymer substrate due to heat load of electron beam. Given that coefficient of thermal expansion of SiO_2 and polymer are significantly different, this may result in change of dimension of polymeric substrate, which might ultimately impact SiO_2 modulus value. Even though this range is extremely wide, we can conclude that true value SiO_2 lies somewhere between 14 GPa and 46 GPa for SiO_2 Type A and between 17 GPa and 58 GPa for SiO_2 Type B. Scherer [15] determined moduli of 120 nm SiO_2 thin film on glass substrate to be between 35 GPa and 48 GPa (SiO_2 deposition by electron-beam evaporation involving introduction of oxygen gas). This is within the range of moduli found for SiO_2 Type A, taking into account standard deviations. Characterization of mechanical properties by AFM were performed using a Peak Force value of 1000 nN, which has been chosen to have a deformation value around 2 nm. Results are summarized in Table 2.

TABLE 2
ELASTIC MODULI OF SiO_2 TYPE A AND B DEPOSITED ON WAFER AND ON OPHTHALMIC LENS, OBTAINED BY AFM

Substrate	Young Modulus (GPa) SiO_2 A	Young Modulus (GPa) SiO_2 B
Silicon Wafer	48±9	64±14
Ophthalmic lens (hardcoat on Polycarbonate)	22±3	23±3

Mean values are calculated for the four sample configurations from 262144 (512x512) approach-retract curves. Modulus of SiO_2 Type B is 33% (48 ± 9 GPa) higher than modulus of SiO_2 Type A (64 ± 14 GPa) on Si wafer when modulus of SiO_2 Type B is 5% (22 ± 3 GPa) higher than modulus of SiO_2 Type A (23 ± 3 GPa) on polymeric lens substrate. Taking into account the high standard deviations values, moduli of SiO_2 A and B on each substrate, could be considered similar. The high standard deviations on moduli values could come from topographic crosslink modifying the effective contact area, resulting in erroneous calculi from DMT model. Roughness (Ra) of SiO_2 film on Si wafer were measured around 2 nm. Topographic cross link remains under study as well as possible mechanical heterogeneities existing in the films at the nanometric scale. On the other hand, SiO_2 moduli on silicon wafer are significantly higher than SiO_2 moduli on ophthalmic lens. This suggests that moduli of thin film are still impacted by substrate, even though deformation depth was found to be roughly 2 nm. Hypothesis can be made on AFM tip's oscillation at 2 kHz, which may affect behavior of viscoelastic hardcoat underneath SiO_2 thin film on lens structure, causing differences observed on moduli between the two substrates.

3.2 Mechanical Adhesion of thin film

3.2.1 Determination of interfacial shear stress by micro-tensile test

Presented on Figure 4 is a Scanning Electron Micrograph of fractured tensile specimens. Inter-crack spacing is clearly defined and averaged over 15 measurements before computing it into Agrawal and Raj's model. Interfacial shear stress ranges from 9 to 14 MPa, due to variability in first cracking occurrence determination and steady state determination

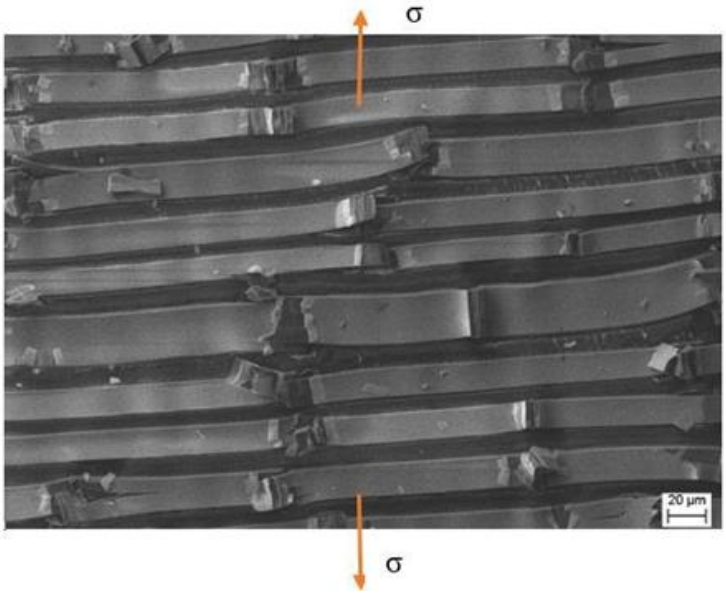

FIG. 4. Scanning Electron Micrograph of fractured tensile specimen

EDS analyses were performed on fractured areas to determine at which interface cracking occurred (Figure 5). Large quantity of carbon in areas where interface is released indicates polycarbonate substrate is underneath cracked layer. This suggests that interface characterized is hardcoat / substrate. Given that SiO_2 thin film is more rigid than underlying hardcoat, it is likely that cracking of SiO_2 appeared before cracking of hardcoat. This seems to indicate that first visible cracking under SEM, occurs in the hardcoat. Characterization under other optical methods which may allow better detection of cracking of SiO_2, will be tested.

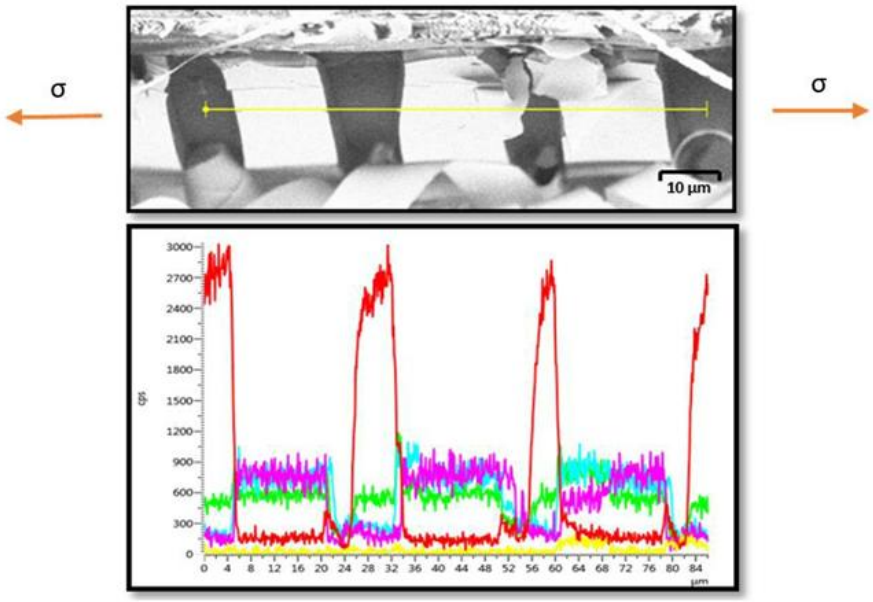

FIG. 5. Scanning Electron Micrograph of delaminated area after micro-tensile test (top image) with EDS profiles over delaminated area: Carbon (red), Oxygen (Green) and Silicon (blue). (bottom image).

3.2.2 Determination of critical stress for onset buckling by micro-compression test

Initiation and instantaneous propagation of buckles, as well as cracking, were observed during application of compressive stress on SiO_2 Type B on lens sample. During the relaxation phase, straight-sided buckles progressively convert to telephone cords morphologies [25]. Concomitance of buckling and cracking (Figure 6) during testing can be explained with hypothesis on mechanisms of their initiations. It is assumed that given sufficient energy, initiation of buckling, followed by its widening, seems to be the logical sequence of events. However, in areas where adhesion is stronger, buckle enlargement seems more difficult than growth of buckle height. This is likely to generate important bending curvatures that eventually lead to cracking. Therefore, we can formulate the hypothesis that occurrence of buckle or cracking can give information on adhesion at a very local level. Ratio of buckles to cracks populations was estimated to be approximately 2 over an observation area of 1.7 x 2.3 mm². Half-width of uncracked buckles averaged over 15 measurements is b = 18±2 µm. This gives values of energy release rates ranging from 0.1 J/m² to 0.5 J/m², depending on moduli values found on wafer or lens substrate. This is within the range of adhesion energies found in the literature, for example, 0.8 to 1.2 J/m² for Au on PI [8]. During relaxation, edges of buckle tend to flatten and end up resting on surface. As relaxation goes on, longitudinal buckle evolves into telephone cord morphology as shown in Figure 7.

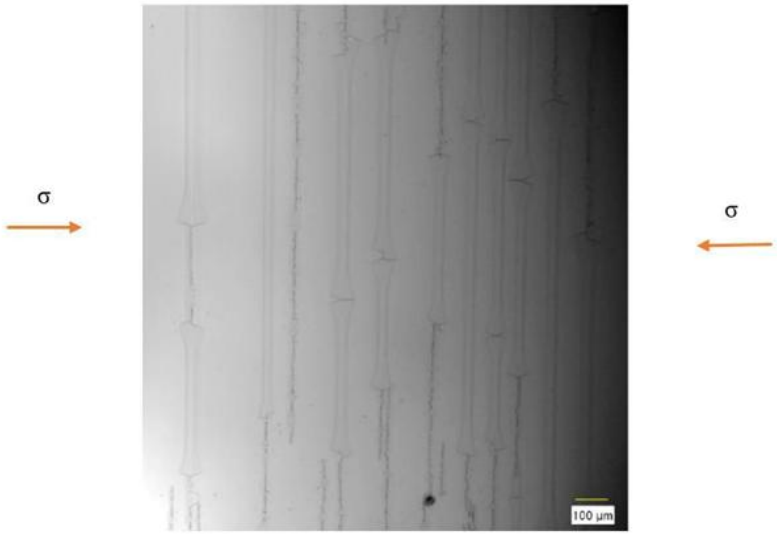

FIG. 6. Optical Microscope observation of buckles and cracks after micro-compression tests. Concomitance of buckles and cracks (x 5). Buckles and transverse cracks (x 20).

Height of buckle under stress could not be measured because in-situ high-resolution topography measurement technique has not been implemented yet. However, height of telephone cord observed in post-mortem specimen was estimated to be 2.2 µm (Figure 7). Identification of layer that buckles has been made on a specimen where telephone cords have been removed by tape, in order to release the interface. Step height of delaminated areas, identified with AFM, was found to be 200 nm which corresponds to thickness of SiO_2. Profile analysis of chemical composition over a delaminated area shows increased quantity of silicon and oxygen and decreased quantity of carbon on higher zones. These analyses strongly suggest delamination at the SiO_2 / Hardcoat interface and support validation of micro-compressive testing as an effective adhesion test to solicit interface of interest.

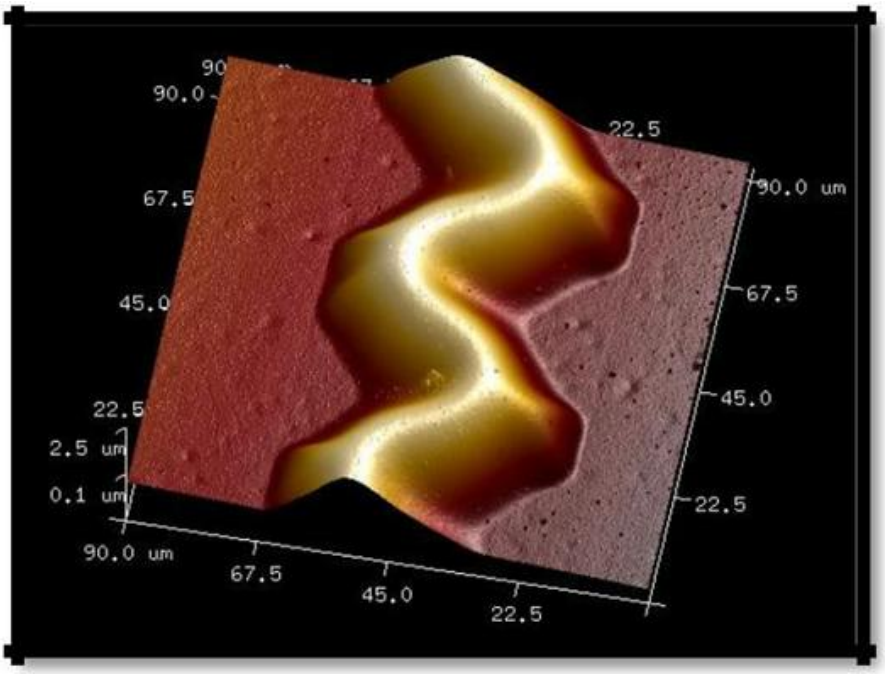

FIG. 7. Telephone cord morphology observed during relaxation of compressive stress, obtained by AFM

IV. CONCLUSION

Elastic moduli of SiO_2 Type A and B were determined by nano-indentation, giving results ranging between 46 and 58 GPa for Si wafer substrate and 14 and 17 GPa for polymeric lens substrate. Same measurements were carried out using AFM. Moduli found are 48 and 64 GPa for Si wafer substrate and 22 and 23 GPa for polymeric lens substrate. Modulus of SiO_2 Type B was found to be roughly 20% higher than SiO_2 Type A, by nano-indentation. Regarding the high standard deviation of moduli measured by AFM, no significant difference between elastic moduli of SiO_2 Type A and B was observed by AFM on both substrates. However, an important difference between moduli of SiO_2 on lens and on Si wafer was observed. This exposes unexpected influence of substrate on mechanical measurements using AFM, which has been hypothetically attributed to impact of Peak Force high frequency oscillations on viscoelastic substrates. Adhesion characterization by micro-tensile experiments gives ultimate shear strengths of interface hardcoat-polycarbonate substrate ranging from 9 to 14 MPa. Detection of cracking of SiO_2 on hardcoat is ongoing. EDX profiles over delaminated area obtained by micro-compressive tests, strengthen the hypothesis that delamination occurred at the interface of interest. This gives values of energy release rates ranging from 0.1 J/m² to 0.5 J/m², depending on moduli values found on wafer or lens substrate. Repeatability and reproducibility studies are undergoing to fully validate this adhesion test. Future immediate perspectives include comparison of energy release rates G for different configurations of SiO_2 thin film. Broader perspectives consist of simulating the micro-compressive adhesion test. Simulation is indeed the only method known to access information such as plastic dissipation or deformation, allowing better analysis of adhesion test

ACKNOWLEDGEMENTS

Financial support for the conduct of this research was provided by Essilor International. The authors would like to acknowledge P. Calba's Materials Advanced Characterization team at Essilor International for their technical support. The authors are also grateful to Bruker's Nano-Surface Division team for performing characterization of moduli by AFM, using PF-QNM on Dimension Icon.

REFERENCES

[1] K.L. Mittal, Adhesion measurement of films and coatings: a commentary, in K.L. Mittal (Eds.), Adhesion measurement of films and coatings, (1995), 1–13.

[2] J. Zheng, S.K. Sitaraman, Fixtureless Superlayer-driven delamination test for nanoscale thin-film interfaces, Acta Materiala. 50 (2002) 441-466.

[3] D. Lau, K. Broderick, M. J. Buehler, and O. Buyukozturk, A Robust Nanoscale Experimental Quantification of Fracture Energy in a Bilayer Material System, Proceedings of the National Academy of Sciences 111, 33 (2014) 11990–11995.

[4] S. Barradas, M. Jeandin, C. Bolis, L. Berthe, M. Arrigoni, M. Boustie, & M. Barbezat, Study of adhesion of PROTAL® copper coating of Al 2017 using the laser shock adhesion test (LASAT). Journal of Materials Science, 39(8), (2004), 2707-2716.

[5] Y. Xiang, X. Chen, and J.J. Vlassak, Plane-strain bulge test for thin films. Journal of materials research 20.09 (2005): 2360-2370.

[6] J. Alexis, C. Gaussens, B. Etcheverry & J. P. Bonino, Development of nickel–phosphorus coatings containing micro particles of talc phyllosilicates. Materials Chemistry and Physics, 137(3) (2013) 723-733.

[7] J. Alexis, C. Gaussens, B. Etcheverry, J-P. Bonino, Development of nickelephosphorus coatings containing micro particles of talc Phyllosilicates, Materials Chemistry and Physics 137 (2013) 723-733.

[8] X. Xue, S. Wang, H. Jia, C. Zheng, H.Bai, Z. Wang, Buckling delamination and cracking of thin titanium films under compression: Experimental and numerical studies, Surface and Coatings Technology, 244 (2014) 151-157.

[9] G.M. Oliver, W.C. Pharr, Improved technique for determining hardness and elastic modulus using load and displacement sensing indentation experiments. Journal of Materials Research, 7 6 (1992) 1564-1583.

[10] H. Li & J. J. Vlassak, Determining the elastic modulus and hardness of an ultra-thin film on a substrate using nanoindentation. Journal of Materials Research, 24(03) (2009) 1114-1126.

[11] J. Hay & B. Crawford, Measuring substrate-independent modulus of thin films. Journal of Materials Research, 26(06) (2011) 727-738.

[12] J. Hopf & E.M. Pierce, Topography and mechanical property mapping of International Simple Glass surfaces with atomic force microscopy. Procedia Materials Science, 7, (2014) 216-222.

[13] P. Trtik, J. Kaufmann, U. Volz, On the use of peak-force tapping atomic force microscopy for quantification of the local elastic modulus in hardened cement paste, Cem. Concr. Res., (42) 1 (2012) pp. 215–221.

[14] P. Roisin, Method for producing an optical article coated with an antireflection or a reflective coating having improved adhesion and abrasion resistance properties, US 8318245 B2 (2012).

[15] K. Scherer, Optical and mechanical characterization of evaporated SiO_2 layers. Long-term evolution, Applied Optics, 35 25, (1996) 5067 – 5072.

[16] G. Stoney, The tension of metallic films deposited by electrolysis, Proceedings of The Royal Society A: Mathematical, Physical and Engineering Sciences, 82 553, (1909) 172-175.

[17] M. Ohring, Materials Science of Thin Films, Second Edition, Elsevier Science, 2001.

[18] J. Barbe, Procédé pour contraindre un motif mince, EP 1615271 B1 (2010).

[19] V. Derjaguin, V. M. Muller et Yu. P. Toporov, Effect of Contact Deformations on the Adhesion of Particles, Journal of Colloid and Interface Science, 53 2 (1975) 314–326.

[20] D. Maugis, Contact Adhesion and Rupture of Elastic Solids, Springer-Verlag Berlin Heidelberg, 2000.

[21] D.C. Agrawal and R. Raj, Measurement of the ultimate shear strength of a metal-ceramic interface, Acta metall., 37 4 (1989) 1265-1270.

[22] Y. Balcaen, N. Radutoiu, J. Alexis, J.-D. Beguin, L. Lacroix, D. Samélor, C. Vahlas, Mechanical and barrier properties of MOCVD processed alumina coatings on Ti6Al4V titanium alloy, Surface and Coatings Technologies, 206 7 (2011) 1684-1690.

[23] M-W. Moon et al. Buckle delamination on patterned substrates. Acta Materialia 52.10 (2004): 3151-3159.